PHILOSOPHICAL TRANSACTIONS OF THE ROYAL SOCIETY A MATHEMATICAL, PHYSICAL & ENGINEERING SCIENCES

Sublithospheric Loading and Plate-Boundary Forces [and Discussion]

M. H. P. Bott, S. Stein, R. Wortel, N. Kusznir, L. Fleitout, M. L. Zoback and J. Cartwright

Phil. Trans. R. Soc. Lond. A 1991 **337**, 83-93
doi: 10.1098/rsta.1991.0108

Sublithospheric loading and plate-boundary forces

By M. H. P. Bott

Department of Geological Sciences, University of Durham, South Road, Durham DH1 3LE, U.K.

Sublithospheric loading arises from anomalous densities in the mantle, such as cool subducting slabs and regions affected by hot spots. Such loading gives rise to isostatic flexure and to tectonic stress in the strong upper lithosphere. Simple models of sublithospheric loading have been studied by finite-element analysis. The maximum loading stress produced by a simple load increases with its width towards the theoretical density-moment function value, but is found to be almost independent of depth for a narrow load (in contrast to a wide load). A layer of low viscosity above the load reduces the stress, depending on its thickness and viscosity.

If the lithospheric stress arising from loading is intersected by a zone or plane of weakness, then plate-boundary tractions develop on the adjacent plates resulting from the redistribution of stress. It is shown, by modelling, that ridge push, slab pull and trench suction can be explained in this way.

1. Introduction

Tectonic stress in the lithosphere must be produced by a source which in general can be renewed as rapidly as it is dissipated by ongoing tectonic activity. The most obvious such source is sublithospheric loading associated with regions of anomalous density in the mantle. The best-known sources of this type include the hot low-density upwelling asthenosphere beneath ocean ridges, the upper mantle hot spots beneath continental and oceanic swells, and cool dense subducting oceanic lithosphere. This paper examines how sublithospheric loading produces tectonic stress in the strong upper lithosphere, and how such stress systems can give rise to plate-boundary forces.

Subsurface loading is usually the primary load in active tectonic regions and may occur within and/or below the lithosphere. The isostatic flexural response of the lithosphere to the deep load produces a secondary topographic load at the surface. Loading stress is produced by a combination of such subsurface and surface loading. Stresses produced by loading are of two types. *Bending stress* results from local asymmetry between the surface and subsurface loads. *Loading stress* without bending occurs when surface and subsurface loads mirror-image each other as in simple local isostatic equilibrium. Flexural isostatic equilibrium gives rise to superimposition of both loading and bending stress. Loading stress concentrates upwards into the strong upper lithosphere and, in contrast to bending stress, its magnitude is inversely proportional to the thickness of the strong upper lithosphere (Kusznir & Bott 1977).

The concept of local isostatic loading stress was discussed qualitatively by Bott (1971, p. 237) and subsequently evaluated across passive margins (Bott & Dean 1972), for more general crustal thickness variations (Artyushkov 1973) and for sublithospheric loading (Bott & Kusznir 1979). For structures which are wide

Phil. Trans. R. Soc. Lond. A (1991) **337**, 83–93
Printed in Great Britain

compared with their depth an approximate estimate of the deviatoric stress σ'_{xx} in an elastic layer of thickness T produced by local isostatic loading can be obtained using the density-moment function (Parsons & Richter 1980; Dahlen 1981)

$$\sigma'_{xx} = \frac{1}{2T}\int_0^D gz\Delta\rho\,\mathrm{d}z, \tag{1}$$

where z is depth below surface, D is depth to base of anomalous density $\Delta\rho$ and g is gravity. The geoid anomaly Δh of a wide structure in local isostatic equilibrium is also proportional to the density-moment function (Haxby & Turcotte 1978)

$$\Delta h = \frac{-2\pi G}{g}\int_0^D z\Delta\rho\,\mathrm{d}z. \tag{2}$$

Thus for very wide loads, the deviatoric loading stress is proportional to the geoid anomaly, and both increase linearly with the depth of the load.

This paper models loading stress in the strong upper lithosphere and associated flexural topography produced by sublithospheric loading, using elastic/viscoelastic finite-element modelling based on the initial strain method. The finite-element package has been developed in the Durham department, with the most substantial input being made by Waghorn (1984). Triangular and quadrilateral isoparametric elements with six and eight nodes respectively are used. Faults can be included using the dual node technique (Goodman *et al.* 1968). The models are run for a sufficient number of time steps for relaxation of the stress in the most viscous region, with time steps being short enough to avoid instability in the least viscous region. The process of approaching dynamic equilibrium in the models is not of geological significance (as it would be for post-glacial uplift studies) as the geological timescale of development of major tectonic structures is much longer.

The modelling assumes the out-of-plane deviatoric stress is zero, as this is most suitable for the viscoelastic creep computation. However, the elastic layer deformation and the in-plane stress differences are almost identical to results obtained with the plane strain formulation. Both the stresses and the flexural uplift are computed. The geoid anomaly can also be computed from the calculated free air gravity anomaly of the models using the fast Fourier transform (FFT) to carry out the transformation in the wavenumber domain. The anomalous densities are referenced to a specified density–depth distribution such as at an edge of the model. The computed stresses can thus be regarded as being superimposed on this standard lithostatic pressure distribution.

2. Simple model of sublithospheric loading

A simple symmetrical two-dimensional finite-element grid extending 3000 km horizontally and down to 700 km depth, neglecting the Earth's curvature, has been used to study sublithospheric loading. An upper elastic layer 25 km thick overlies a substratum with viscosity of 10^{21} Pa s. The resulting stresses, however, are independent of the viscosity although the relaxation time is proportional to viscosity. Young's modulus and Poisson's ratio are 1.75×10^{11} Pa and 0.27 respectively throughout. The flexural rigidity of the elastic layer is 2.46×10^{23} N m which is near the middle of the continental range (Walcott 1970). For the purpose of applying isostatic restoring forces, a mantle density of 3330 kg m^{-3} has been assumed. The load consists of a 100 km × 100 km region of square cross section with

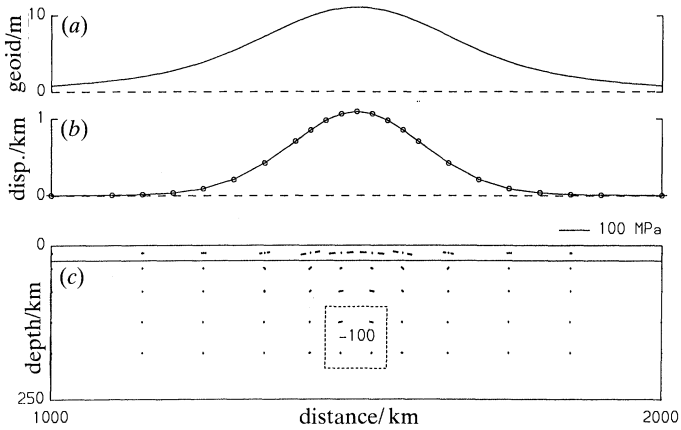

Figure 1. The deviatoric stress distribution (*c*), surface elevation profile (*b*) and geoid anomaly (*a*) at 20 km height resulting from the two-dimensional $-100\ \mathrm{kg\ m^{-3}}$ region of anomalously low density outlined by the broken line. The solid line denotes the base of the 25 km thick elastic layer. The in-plane deviatoric stress nearest to the horizontal is shown, with a thick broken line denoting tension and (in other figures) a thick unbroken line denoting compression.

an anomalous density of $-100\ \mathrm{kg\ m^{-3}}$ relative to the normal mantle, situated beneath the centre of the symmetrical model. The stresses and surface displacements would be equal but of opposite sign for an equivalent positive density anomaly. The average deviatoric stress nearest to the horizontal is shown at the centre of each element (the other in-plane deviatoric stress is equal but opposite). Thus the small bending stresses are eliminated as the elastic layer is one element thick.

Model SLLA (figure 1), with the centre of the load at 150 km depth, has been run for 200 time steps of 500 years each (totally 100 000 years) to enable the shape of the uplift produced by the load to develop almost fully. The main features are (1) a flexural uplift reaching a maximum of 1028 m, (2) a free air geoid anomaly of 11.05 m maximum relative to the value at the distant edges, and (3) deviatoric stresses which have relaxed to small values in the viscous region but have concentrated up into the strong elastic layer reaching a maximum value of 78 MPa at the centre. This model demonstrates in a simple way the effectiveness of a sublithospheric load in causing vertical isostatic displacement at the surface and in stressing the strong upper lithosphere. The timescale for this to occur is much shorter than that required to dissipate the load by advection. However, because of the finite lateral extent of the load, the geoid maximum is only 17 % of the theoretical value from equation (2) and the maximum deviatoric stress is only 27 % of the theoretical value from equation (1).

Figure 2 illustrates how the deep load in figure 1 couples to the strong lithosphere. The load gives rise to an anomalous pressure field above it which acts on the base of the elastic layer to produce the flexural uplift. Part of the deviatoric stress in the layer is produced by this pressure and that of the surface topography, but most of it arises from the outwardly directed shear traction exerted by the advecting viscous material driven by the load.

The variation of maximum height, maximum geoid anomaly and maximum deviatoric stress is shown in figure 3*a* as a function of width/depth ratio, with the

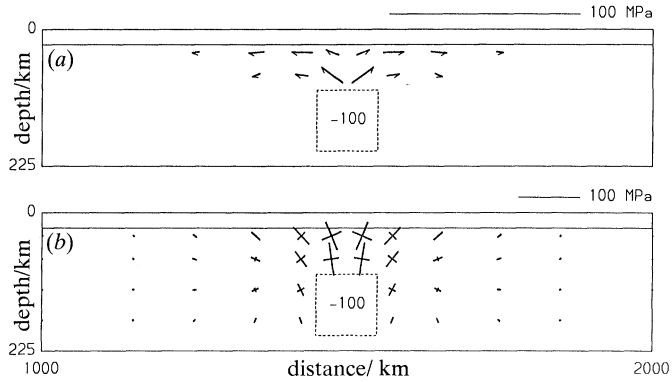

Figure 2. The element-averaged compressional principal stress (*b*) and shear stress (*a*) in the viscoelastic region beneath the elastic layer for Model SLLA (figure 1), demonstrating the anomalous normal pressure and shear stress applied to the base of the elastic layer as a result of the deep load.

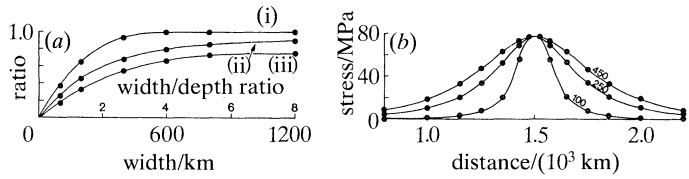

Figure 3. (*a*) The maximum values of deviatoric stress, surface elevation and geoid anomaly as ratios to the values for an infinitely wide structure, plotted against width (and width/depth ratio) for a 100 km thick load centred at 150 km depth as in Model SLLA, but of varying width. (i) Height; (ii) stress; (iii) geoid. (*b*) The profile of element-averaged deviatoric stress in the elastic layer for models similar to SLLA but with varying depth to the centre of the load. Depth is shown in kilometres above the profiles.

load of Model SLLA being progressively widened. These loads are all centred at 150 km depth and are 100 km thick. Figure 3*a* shows that the maximum elevation increases rapidly with width/depth ratio towards the local isostatic value, and the maximum deviatoric stress and geoid anomaly tend rather more gently towards the theoretical values given by equations (1) and (2). The effect of varying the depth of the simple square load of Model SLLA on the distribution of stress is shown in figure 3*b*. The variation of load depth has almost insignificant effect on the maximum stress value. The width of the stressed region increases approximately linearly with load depth, as might be anticipated.

The effect of a low viscosity layer above the load has been explored in a preliminary way. (i) Model SLLA was modified by reducing the viscosity of the load by a factor of 100. This has a negligible effect. (ii) a 25 km thick layer of reduced viscosity was additionally incorporated immediately above top of the load. For a viscosity reduced by a factor of $\times 100$ the maximum deviatoric tension is 56 MPa and for reduction by $\times 400$ it is 49 MPa (a reduction of about 35%). For loading at this sort of depth, typical for an upper mantle hot spot, the reduction in the stress appears to be significant but not overwhelming. (iii) a reduction of viscosity by a factor of $\times 100$ was next applied to a layer above a deep-seated load centred at 350 km depth. The layer was varied in thickness from 25 to 225 km, with the stress in the upper elastic lithosphere being reduced by about 40–45% in all the models.

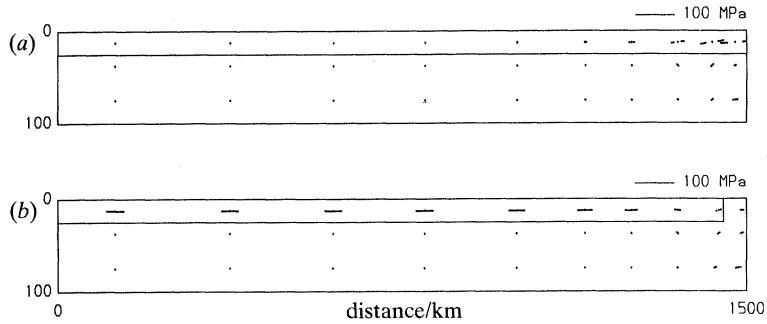

Figure 4. Comparison of the deviatoric stresses in Model SLLA (*a*) with those developed when the model is modified in (*b*) by including a weak crest as shown and constraining the distant edge nodes of the elastic layer to zero horizontal displacement. Note that only one half of the symmetrical models, from the far left edge to the centre, is shown. Vertical exaggeration is $\times 2$.

3. Loading stress and plate-boundary force

Large loading stress might be expected to occur at plate boundaries where prominent sublithospheric loading occurs, such as low-density asthenospheric upwelling beneath ocean ridges and dense sinking slabs beneath subduction plate boundaries. If these boundaries could be strong enough to withstand the loading stress, ridges would be associated with large local extensional stress distributions and subduction zones with large compressions. How, then, do the plate-boundary forces of apparently opposite polarity develop at these boundaries?

This is explained in principle by reference to Model SLLA and its modification shown in figure 4. This diagram shows the shallower part of the left-hand half of the symmetrical models out to their left edge. In figure 4*a* Model SLLA has a continuous elastic layer as in figure 1. In figure 4*b* the model is modified in two ways. First, the central two elastic elements of the symmetrical model have been replaced by viscous elements extending up to the surface to simulate a weak crest. Second, the left edge nodes of the elastic layer have been constrained to zero horizontal displacement.

If the edge is fixed without weakening the crest (not shown), then a small compression occurs out to the fixed edge as expected. If the crestal region is also weakened as shown, then the tensions in the vicinity of the crest are greatly reduced and large compression occurs beyond the central region and extends out to the fixed edge. The effect of weakening the crest is to redistribute the stress throughout the elastic plate by superimposing a large supplementary compression which is slightly smaller than the maximum tension in the unweakened model. The small residual tensions in the vicinity of the weakened crest are associated with the ongoing viscous deformation at the crest, and can be regarded as the plate-boundary resistance. The low-density load thus gives rise to a compressional stress slightly smaller than the local extensional stress of the unweakened model. This extends out to the fixed edge of the plate. If there is viscous drag on the underside of the elastic plate, then this compressional stress will decrease with increasing distance from the plate boundary.

The stress redistribution results from the modified normal pressure acting on the vertical edge of the elastic plate adjacent to the weak element. The plate boundary force, however, can be regarded as arising partly from this increased pressure and partly from the shear traction acting on the base of the nearby part of the elastic

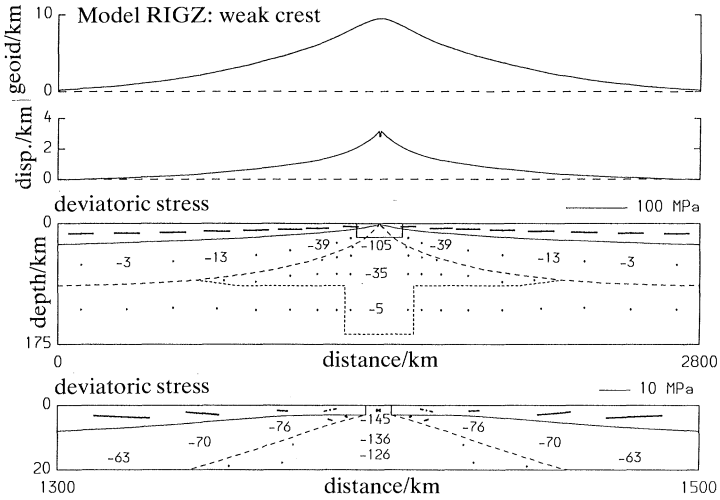

Figure 5. A model of a symmetrical ocean ridge spreading at 15 mm a^{-1} with loading of thermal origin below and within the cooling lithosphere (see text), showing deviatoric stress (enlarged central region below), flexurally developed surface elevation, and geoid anomaly at 20 km height. Anomalous density values as shown are in kg m^{-3} and are referenced to the values at the same depth beneath the old ocean floor at the edges. The base of the elastic lithosphere is marked by the solid line and the base of the seismological lithosphere by the coarse broken line. Vertical exaggeration is $\times 3$ for the full length section.

layer as shown in figure 2. For a deep load such as in Model SLLA, the shear traction effect is strongly dominant.

The plate boundary force, referenced to the normal density–depth profile at the edge, can be determined by integrating the stress difference across the thickness of the elastic layer at the edge. The deviatoric compressional stress at the left edge is 46 MPa, corresponding to a plate-boundary force of 2.3×10^{12} N m^{-1}.

Ridge push

Model RIGZ (figure 5) illustrates the origin of the ridge push force. This model is of a type discussed by Bott (1991), to which reference should be made for further detail. It represents a symmetrical ocean 2800 km wide spreading at 15 mm a^{-1}. The grid extends to 400 km depth with the basal nodes being free. The lithospheric structure is based on the cooling plate model of Parsons & Sclater (1977) and the elastic thickness model of Watts (1978). The thicknesses of the elastic upper lithosphere and the high-viscosity lower lithosphere (10^{23} Pa s) increase from the ridge crest accordingly. The asthenosphere below has an assumed viscosity of 10^{21} Pa s. The density structure as inferred from the temperature field is referenced to 90 Ma oceanic lithosphere at the edges. The uniform oceanic crust is not included, so that the density is taken to increase by 2300 kg m^{-3} at the sea floor for isostatic purposes.

The weak crest is simulated by assigning an asthenospheric viscosity to the two adjacent shallowest elements. The enlargement of the crestal region (below in figure 5) shows that there is a small subhorizontal deviatoric tension near the crest, representing ridge resistance. The stresses become compressional at a small distance from the crest, rapidly increasing to nearly 40 MPa which is maintained to the edges.

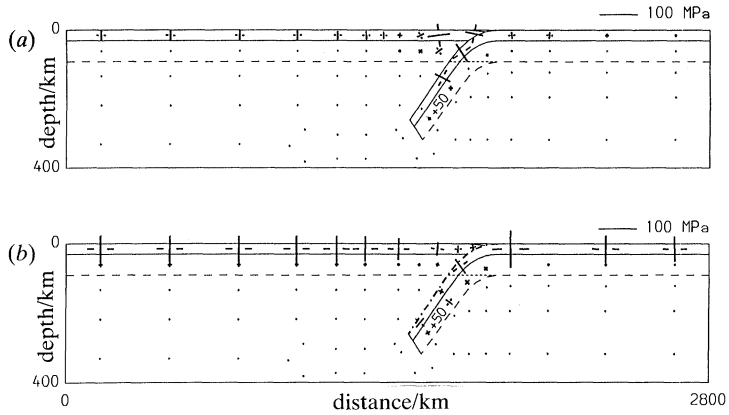

Figure 6. Deviatoric stress distributions produced by (*a*) Model SLA1 (subduction fault locked) and (*b*) Model SLA2 (subduction fault free), with a 45° slab extending to about 300 km depth. Details as in figure 5 and as described in the text. Vertical exaggeration is $\times 1.5$.

The compression is approximately constant over most of the flanking regions because of the trade-off of increasing elastic layer thickness with increasing tectonic force.

The model develops an isostatic elevation of 3.2 km relative to the old ocean floor. The geoid maximum relative to the old ocean is 9.5 m, compared to the theoretical value of 11.7 m calculated for an infinitely wide structure using equation (2). The ridge-push force developed at the fixed edges is 2.43×10^{12} N m^{-1} compared with the theoretical value of 2.69×10^{12} N m^{-1} using equation (1). The discrepancies between the modelled and theoretical values of the stress field and the geoid are much smaller than those discussed in the previous section of the paper because the anomalous density structure is much wider compared with its depth. The ridge resistance slightly reduces the plate-boundary force.

The above estimate of ridge-push force is in good agreement with other estimates (Dahlen 1981; Fleitout & Froidevaux 1983). Bott (1991) has shown that about double this ridge-push force should develop as a result of such a ridge being underlain by an anomalously hot upper mantle with an average temperature anomaly of 70 K down to 400 km depth, which is typical for a hot spot region such as parts of the North Atlantic.

Slab pull and trench suction

Loading stresses associated with subduction and the related plate-boundary forces have been modelled by Bott *et al.* (1989) and by Whittaker *et al.* (1991). Two of the models shown by Whittaker *et al.* (1991) have been replotted in horizontally extended form in figure 6. The model is 2800 km wide and extends to 650 km depth, with vertically fixed nodes at the base. The 45° dipping slab extends to nearly 300 km depth and has an anomalous density of $+50$ kg m^{-3} representing a temperature about 500 K lower than that of the adjacent normal upper mantle. The nodes at both edges of the lithosphere are constrained to zero horizontal displacement so that the force exerted by the subduction system can be determined.

The 90 km thick lithosphere consists of an upper 30 km thick elastic layer overlying a stiff lower part with viscosity of 5×10^{22} Pa s. Oceanic crust is not included, but there is 30 km thick continental crust on the overriding plate with a deficient density of -400 kg m^{-3} relative to the mantle, in local isostatic equilibrium with elevated topography relative to the ocean floor which is simulated by a surface

load. In the continental crust, Young's modulus is 0.9×10^{11} Pa and Poisson's ratio is 0.25. Otherwise the mechanical properties are as in the previous models except that viscosity is higher by a factor of ten below 400 km representing a downward increase at the mantle transition zone. The upper surface of the subducting slab is a fault which can be either locked or unlocked. Further details of the models are given by Whittaker *et al.* (1991).

Model SLAB1 shows the deviatoric stresses which develop after relaxation over 250000 years when the subduction fault is locked. The slab is approaching equilibrium apart from ongoing rollback. Downdip deviatoric tension occurs in the slab, dying off to about zero at the base. The overriding plate above the slab is characterized by large subhorizontal deviatoric compressions of up to about 70 MPa caused by the sublithospheric loading of the dense slab. A small deviatoric tension of 25 MPa extends to the edge, representing the loading stress of the continental crust. The compressional stresses associated with sublithospheric loading die off away from the region underlain by the slab and are small at both edges of the lithosphere.

Model SLAB2 shows the effect of unlocking the fault, which is assigned zero friction. The slab is still sinking and rolling back in this model, and the resistance at the base gives rise to downdip compression which gives way upwards to downdip tension, as is commonly observed in some subducting slabs (Isacks & Molnar 1971). The effect of separating the two plates by a plane of weakness represented by the subduction fault is to superimpose an extensional stress which extends out to the fixed edges of both plates. The deviatoric tension at the edge of the subducting plate is 65 MPa, and at the edge of the overriding plate it is 70 MPa including the 25 MPa from continental crustal loading.

In Model SLAB2, the subducting system is pulling both plates towards the subduction zone, causing plate interior tension in this isolated situation. Integrating the stresses across the lithosphere at the edges of the model, after allowing for the continental crustal loading stress, yields estimates of the plate-boundary forces referenced to old ocean floor as follows. The slab pull force is -4.8×10^{12} N m^{-1} and the trench suction is -4.2×10^{12} N m^{-1}, these being of comparable magnitude as might be expected from the equilibrium of the system.

Whittaker *et al.* (1991) additionally studied vertically dipping slabs, slabs extending to 400 km depth, and the influence of a back-arc basin. In general, the dip of the slab does not greatly affect the plate-boundary forces but they increase with increasing depth extent of the slab. These models all show that slab pull and trench suction originate from the intersection of the compressional loading stress caused by the dense sinking slab by the weak subduction fault. The modification to the boundary tractions on both sides of the fault plane required to annihilate the shear stress gives rise to both local vertical deformation associated with the fault and to the pervasive tensional stresses which extend into the plate interiors.

4. Summary and conclusions

A simple model of sublithospheric loading consisting of a 25 km thick elastic layer above a uniform viscous substratum has been studied by elastic/viscoelastic finite-element analysis. The load is a 100 km × 100 km region of anomalously low density initially centred at 150 km depth. This load causes flexural isostatic uplift and horizontal extensional deviatoric stress in the elastic layer. The stress resulting from

PHILOSOPHICAL TRANSACTIONS OF THE ROYAL SOCIETY A MATHEMATICAL, PHYSICAL & ENGINEERING SCIENCES

the loading is applied to the base of the elastic layer by a combination of excess normal pressure above the load and outwardly directed viscous drag exerted by the advecting viscous material.

Widening the load causes the deviatoric loading stress and the geoid anomaly to increase towards the values given by the density-moment function. Deepening the compact square load has an insignificant effect on the maximum deviatoric stress but the stressed region widens approximately proportionally to the depth of the load. A two-order of magnitude reduction of viscosity of a layer above the load reduces the deviatoric stress by up to 50%.

If the two central elastic elements are made viscoelastic and the edge elastic nodes are fixed horizontally, the sublithospheric loading gives rise to much reduced tension in the crestal region and compression beyond the region of the load. A plate-boundary force akin to ridge push develops resulting from the redistribution of stress. It is demonstrated how this principle applies to a thermal model of a slow spreading ocean ridge, with weak tension occurring beneath the crest and deviatoric compression of about 40 MPa beneath the older ocean floor. The ridge push referenced to old ocean floor is 2.4×10^{12} N m^{-1} and the geoid anomaly is 9.5 m, these being only 10% and 20% respectively below the density-moment function values because the load is wide compared to its depth.

A model of a 45° dipping dense subducting slab extending to about 300 km depth produces large near-horizontal compressional deviatoric stresses in the overriding plate above the slab when the subduction fault is locked. When the fault is unlocked, radical redistribution of stress occurs in the elastic upper lithosphere, with tension developing out to the plate edges when these are fixed horizontally. The slab pull force is determined as -4.8×10^{12} N m^{-1} and the trench suction force as -4.2×10^{12} N m^{-1} for this model.

The computations and manuscript have been produced using the facilities of the Durham University Computer Centre, for which the author is grateful.

References

Artyushkov, E. V. 1973 Stresses in the lithosphere caused by crustal thickness inhomogeneities. *J. geophys. Res.* **78**, 7675–7708.

Bott, M. H. P. 1971 *The interior of the Earth.* London: Edward Arnold.

Bott, M. H. P. 1991 Ridge push and associated plate interior stress in normal and hot spot regions. *Tectonophys.* (In the press.)

Bott, M. H. P. & Dean, D. S. 1972 Stress systems at young continental margins. *Nature, Lond.* **235**, 23–25.

Bott, M. H. P. & Kusznir, N. J. 1979 Stress distributions associated with compensated plateau uplift structures with application to the continental splitting mechanism. *Geophys. Jl R. astr. Soc.* **56**, 451–459.

Bott, M. H. P., Waghorn, G. D. & Whittaker, A. 1989 Plate boundary forces at subduction zones and trench-arc compression. *Tectonophys.* **170**, 1–15.

Dahlen, F. A. 1981 Isostasy and the ambient state of stress in the oceanic lithosphere. *J. geophys. Res.* **86**, 7801–7807.

Fleitout, L. & Froidevaux, C. 1983 Tectonic stresses in the lithosphere. *Tectonics* **2**, 315–324.

Goodman, R. E., Taylor, R. L. & Brekke, T. L. 1968 A model for the mechanics of jointed rock. *J. Soil Mech. Fdns Div. Am. Soc. civ. Engrs* **94**, 637–658.

Haxby, W. F. & Turcotte, D. L. 1978 On isostatic geoid anomalies. *J. geophys. Res.* **83**, 5473–5478.

PHILOSOPHICAL TRANSACTIONS OF THE ROYAL SOCIETY A MATHEMATICAL, PHYSICAL & ENGINEERING SCIENCES

Isacks, B. & Molnar, P. 1971 Distribution of stresses in the descending lithosphere from a global survey of focal-mechanism solutions of mantle earthquakes. *Rev. Geophys.* **9**, 103–174.

Kusznir, N. J. & Bott, M. H. P. 1977 Stress concentration in the upper lithosphere caused by underlying visco-elastic creep. *Tectonophys.* **43**, 247–256.

Parsons, B. & Richter, F. M. 1980 A relation between the driving force and geoid anomaly associated with mid-ocean ridges. *Earth planet. Sci. Lett.* **51**, 445–450.

Parsons, B. & Sclater, J. G. 1977 An analysis of the variation of ocean floor bathymetry and heat flow with age. *J. geophys. Res.* **82**, 803–827.

Waghorn, G. D. 1984 *Numerical modelling of the stress regime at subduction zones.* Ph.D. thesis, University of Durham, Durham.

Walcott, R. I. 1970 Flexural rigidity, thickness, and viscosity of the lithosphere. *J. geophys. Res.* **75**, 3941–3954.

Watts, A. B. 1978 An analysis of isostasy in the world's oceans. 1. Hawaiian–Emperor seamount chain. *J. geophys. Res.* **83**, 5989–6004.

Whittaker, A., Bott, M. H. P. & Waghorn, G. D. 1991 Stresses and plate boundary forces associated with subduction plate margins. *J. geophys. Res.* (In the press.)

Discussion

S. Stein (*Northwestern University, Evanston, U.S.A.*). Has Professor Bott tried to couple the continental-rift-style model with the zone of extension because the extension zone in East Africa is about a 1000 miles across as opposed to about 10 km for a mid-ocean ridge?

M. H. P. Bott. In East Africa the eastern and western rift systems are narrow and are separated by a wide cratonic region which is not undergoing extension.

R. Wortel (*Utrecht University, The Netherlands*). If I remember correctly the model of the Alps with the root was proposed by Müller and colleagues on the basis of seismic velocity information which they inferred from the propagation of seismic surface waves and I am not aware of any information about the root being detached from the surface.

M. H. P. Bott. The deep lithospheric root beneath the Alps has been inferred from both seismological and gravity evidence, and is also implied by the plate convergence. It appears to be attached to the lithosphere above but in reality is presumably separated from the strong upper lithosphere by ductile lower lithosphere as in the models.

N. Kusznir (*Liverpool University, U.K.*). Has Professor Bott modelled the net effect of the transition from continent to ocean where there is a substantial density contrast at depth? Is there any consensus from geoid information as to what happens as one goes from continent to ocean?

M. H. P. Bott. The ocean ridge models shown do not include a denser subcontinental mantle, although such may exist and would have the effect of increasing the compressional stress in the continental region. This should be reflected in the geoid anomaly, and L. Fleitout, who has worked on this problem, may wish to comment further.

L. Fleitout (*École Normale Supérieure, Paris, France*). I think it depends on the particular passive margin. I think the first work in this field was done by Turcotte and others who commented that there was no change in the geoid as one crossed passive margins. I have looked at that problem recently and it is true that on many, though not all passive margins, there is not a visible geoid jump across the boundary.

S. Stein (*Northwestern University, Evanston, U.S.A.*). On a lot of passive margins people have estimated that the flexural stresses that one gets from the sediments are enormous and I am curious to know how rapidly these sorts of forces would dissipate. Has Professor Bott calculated how these forces would drop off towards the interior of a continent?

N. Kusznir (*Liverpool University, U.K.*). The bending stresses due to sedimentation at continental margins are very large and calculations suggest that brittle failure should occur. I think there is evidence for the large bending stresses and brittle failure because the effective elastic thicknesses that we see for such systems are very small and are quite unlike, for example, ocean basin thicknesses. I think one of the reasons the effective elastic thicknesses are so thin is that bending stresses have generated failure. Why don't we get earthquakes? Could this be due to the fact that bending stresses are non-renewable?

M. H. P. Bott. I agree that the non-renewable nature of bending stresses may account for the lack of earthquakes associated with plate interior bending stress.

M. L. Zoback (*US Geological Survey, Menlo Park, U.S.A.*). There is some relevant data. We know the orientation of the margins so presumably we can know the orientation of the extensional stresses due to sediment loading and the extensional stresses due to the density contrast between crust and mantle.

J. Cartwright (*Imperial College London, U.K.*). To get the stresses necessary for extension on a continental-rift scale in your models, with the wavelength you showed, you always had a topographic effect of between 1 and 2 km. Is there any situation that can be envisaged for major continental rifts without that topographic effect on their shoulders? If there is a flat borderland to the rift, what would be the stresses for that sort of condition?

M. H. P. Bott. Yes, the rift systems of interplume passive margins and of the North Sea differ from the uplifted Tertiary continental rift systems in being formed at low elevation. Extensional stress of distant origin, such as from plate-boundary forces, was presumably the cause of these low-lying rift systems, in contrast to the main Tertiary rift systems.

PHILOSOPHICAL TRANSACTIONS OF THE ROYAL SOCIETY A MATHEMATICAL, PHYSICAL & ENGINEERING SCIENCES